Cell Reports
Methods

Report

Direct capture of neutralized RBD enables rapid point-of-care assessment of SARS-CoV-2 neutralizing antibody titer

Graphical abstract

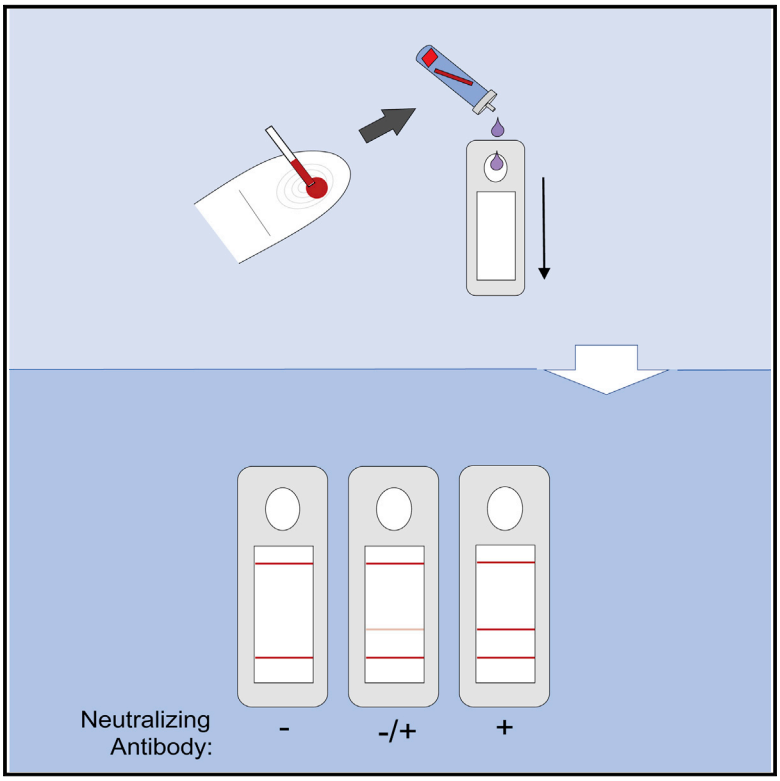

Authors

Guinevere G. Connelly, Orville O. Kirkland, Seven Bohannon, ..., Sangeeta N. Bhatia, Hadley D. Sikes, Hojun Li

Correspondence

hojunli@mit.edu

In brief

Connelly et al. developed a lateral flow methodology for quantifying SARS-CoV-2 neutralizing antibody titer. This workflow is compatible with point-of-care or at-home testing from a capillary blood sample without laboratory equipment. Diagnostic accuracy was confirmed for a wide range of neutralizing antibody titers collected from naive, convalescent, and immunized patients.

Highlights

- Lateral flow assay detecting SARS-CoV-2 neutralizing antibodies
- Quantification of antibody titer from capillary blood sample
- Rapid workflow compatible with point-of-care and at-home usage
- Diagnostic performance validated with naive, convalescent, and vaccinated patients

Connelly et al., 2022, Cell Reports Methods 2, 100273
August 22, 2022
https://doi.org/10.1016/j.crmeth.2022.100273

CellPress

Cell Reports Methods

CellPress
OPEN ACCESS

Report

Direct capture of neutralized RBD enables rapid point-of-care assessment of SARS-CoV-2 neutralizing antibody titer

Guinevere G. Connelly,[1,19] Orville O. Kirkland,[1,19] Seven Bohannon,[2] Daniel C. Lim,[1] Robert M. Wilson,[1,3] Edward J. Richards,[1,4] Dousabel M. Tay,[5] Hyuk Jee,[6] Riley D. Hellinger,[1] Ngoc K. Hoang,[1] Liang Hao,[1] Arnav Chhabra,[1,7] Carmen Martin-Alonso,[1] Edward K.W. Tan,[1] Angela N. Koehler,[1,3,8] Michael B. Yaffe,[1,3,9] Wendy B. London,[10,11,12] Pui Y. Lee,[6,12] Florian Krammer,[13] Robert C. Bohannon,[2] Sangeeta N. Bhatia,[1,8,14,15,16,17,18] Hadley D. Sikes,[5] and Hojun Li[1,10,11,12,20,*]

[1]Koch Institute for Integrative Cancer Research, Massachusetts Institute of Technology, Cambridge, MA 02139, USA
[2]Catalloid Products, Elkhart, IN 46514, USA
[3]Department of Biological Engineering, Massachusetts Institute of Technology, Cambridge, MA 02139, USA
[4]Dragonfly Therapeutics, Waltham, MA 02451, USA
[5]Department of Chemical Engineering, Massachusetts Institute of Technology, Cambridge, MA 02139, USA
[6]Division of Rheumatology, Boston Children's Hospital, Boston, MA 02115, USA
[7]Satellite Bio, Cambridge, MA 02139, USA
[8]Broad Institute of MIT and Harvard, Cambridge, MA 02142, USA
[9]Department of Biology, Massachusetts Institute of Technology, Cambridge, MA 02139, USA
[10]Division of Hematology/Oncology, Boston Children's Hospital, Boston, MA 02115, USA
[11]Department of Pediatric Oncology, Dana-Farber Cancer Institute, Boston, MA 02215, USA
[12]Harvard Medical School, Boston, MA 02115, USA
[13]Department of Microbiology, and Department of Pathology, Molecular and Cell Based Medicine, Icahn School of Medicine at Mount Sinai, New York, NY 10029, USA
[14]Harvard-MIT Division of Health Sciences and Technology, Cambridge, MA 02139, USA
[15]Institute for Medical Engineering and Science, and Electrical Engineering and Computer Science, Massachusetts Institute of Technology, Cambridge, MA 02139, USA
[16]Department of Medicine, Brigham and Women's Hospital, Boston, MA 02115, USA
[17]Howard Hughes Medical Institute, Cambridge, MA 02139, USA
[18]Wyss Institute at Harvard, Boston, MA 02115, USA
[19]These authors contributed equally
[20]Lead contact
*Correspondence: hojunli@mit.edu
https://doi.org/10.1016/j.crmeth.2022.100273

MOTIVATION A major component of protective immunity against SARS-CoV-2 infection is the presence of neutralizing antibodies that can block viral infection of host cells when present at high titer. Following SARS-CoV-2 infection or spike protein mRNA vaccination, high-titer neutralizing antibody titers do not persist long term, and consequently, immunity wanes. Methods for measuring neutralizing antibodies against SARS-CoV-2 typically require laboratory processing and specialized personnel. Thus, we sought to develop a methodology capable of quantifying SARS-CoV-2 neutralizing antibody titer at the point of care or at home.

SUMMARY

Neutralizing antibody (NAb) titer is a key biomarker of protection against severe acute respiratory syndrome coronavirus 2 (SARS-CoV-2) infection, but point-of-care methods for assessing NAb titer are not widely available. Here, we present a lateral flow assay that captures SARS-CoV-2 receptor-binding domain (RBD) that has been neutralized from binding angiotensin-converting enzyme 2 (ACE2). Quantification of neutralized RBD in this assay correlates with NAb titer from vaccinated and convalescent patients. This methodology demonstrated superior performance in assessing NAb titer compared with either measurement of total anti-spike immunoglobulin G titer or quantification of the absolute reduction in binding between ACE2 and RBD. Our testing platform has the potential for mass deployment to aid in determining at population scale the degree of protective immunity individuals may have following SARS-CoV-2 vaccination or infection and can enable simple at-home assessment of NAb titer.

INTRODUCTION

A major aspect of global efforts to curtail the coronavirus disease 2019 (COVD-19) pandemic involves ensuring that the majority of individuals in the population have protective immunity against severe acute respiratory syndrome coronavirus 2 (SARS-CoV-2). Protective immunity generated after either active infection or vaccination can wane over time, resulting in loss of protection against infection and disease (Collier et al., 2021; Goldberg et al., 2021). Although both humoral and cellular immunity contribute to protective immunity against SARS-CoV-2, a well-established biomarker for protective immunity that predicts susceptibility to infection is neutralizing antibody (NAb) titer (Gilbert et al., 2022; Khoury et al., 2021; Krammer, 2021).

Several robust methodologies exist for measuring SARS-CoV-2 NAb titer in the laboratory setting. These include live-virus neutralization assays (Amanat et al., 2020b; Bewley et al., 2021; Manenti et al., 2020), spike protein pseudotyped viral (pseudoviral) neutralization assays (Bewley et al., 2021; Crawford et al., 2020; Nie et al., 2020), and enzyme-linked immunosorbent assays (ELISA) measuring inhibition of the binding interaction between spike protein receptor-binding domain (RBD) and the extracellular domain (ECD) of angiotensin-converting enzyme 2 (ACE2) (Tan et al., 2020), the principal SARS-CoV-2 cell-surface receptor (Letko et al., 2020; Wrapp et al., 2020; Yan et al., 2020). These methodologies require centralized processing and trained personnel with specialized equipment, making them incompatible with mass deployment for point-of-care NAb titer assessment in the general population. Although anti-spike and anti-RBD antibody levels measured by ELISA correlate with NAb titer (Yun et al., 2021), existing point-of-care assays for anti-spike and anti-RBD antibodies have insufficient sensitivity and specificity and are likely of limited diagnostic utility in assessing true NAb status in individuals (Lisboa Bastos et al., 2020). Creation of a field-deployable test for rapid assessment of SARS-CoV-2 NAb titer has the potential to be transformative in population-scale efforts to curb the spread of SARS-CoV-2. Such a test would allow individuals to know on any given day what degree of NAb protection they have circulating in their bloodstream. Furthermore, a field-deployable test would allow for large-scale studies to identify the NAb titers that confer protection against SARS-CoV-2 infection (Krammer, 2021). To address this unmet need, we developed a lateral flow assay (LFA) that quantifies the amount of RBD unable to bind ACE2 due to neutralization by patient plasma. This LFA demonstrates robust performance in predicting NAb titer in individuals following either SARS-CoV-2 vaccination or natural infection.

RESULTS

To develop a methodology for assessing circulating NAb titer in a rapid manner at the point of care, we reasoned that neutralization of RBD:ACE2 binding (Figures 1A and 1B) should serve as a core component since ELISA-based measurement of neutralization of RBD:ACE2 binding is a validated metric correlating with NAb titer (Nandakumar et al., 2021; Tan et al., 2020). However, a weakness of relying on solely measuring a reduction in binding signal is the potential for the assay to have limited dynamic range. This is overcome in laboratory-based assays by testing serial dilutions of a sample, but this approach is incompatible with point-of-care and at-home testing. To address this issue, we engineered a testing method that produces a positive signal in the presence of NAbs; this positive signal also facilitates greater ease of use and interpretation, which are paramount for successful implementation of a diagnostic test in the at-home setting (Murray and Mace, 2020). In this method, RBD molecules neutralized by NAbs are unable to bind ACE2 and are subsequently captured downstream in an LFA (Figure 2A).

We first generated two 293T cell lines stably secreting either recombinant RBD or a fusion protein consisting of ACE2 ECD linked with a cellulose-binding domain (hereafter referred to as ACE2-CBD) for attachment to a cellulose or nitrocellulose test strip (Miller et al., 2018). Both protein constructs possessed affinity tags and could be generated with good purity (Figures 1C and S1A). To validate that recombinant RBD and ACE2-CBD could bind to each other, varying amounts of ACE2-CBD were spotted onto cellulose strips, incubated with soluble RBD, and the amount of RBD bound to each ACE2-CBD spot was detected using an anti-RBD monoclonal antibody (CR3022) (Huo et al., 2020). These experiments demonstrated that RBD could bind to cellulose-immobilized ACE2-CBD and that binding was blocked by a commercial recombinant monoclonal NAb isolated from a patient naturally infected with SARS-CoV-2 (Figures 1D and 1E).

To determine if RBD:ACE2 binding could occur in a lateral flow format, we next spotted ACE2-CBD on a cellulose test strip and applied RBD diluted in pre-pandemic human plasma to one end of the test strip (Figure 1F). After 15 min of lateral flow runtime, we detected RBD bound to ACE2 using the CR3022 monoclonal anti-RBD antibody. As shown in Figures 1G and 1H, RBD could bind ACE2 in a lateral flow format, and that binding was blocked when RBD was pre-mixed with the commercial monoclonal NAb.

We then generated prototype LFA test cassettes comprised of a nitrocellulose strip containing a line of immobilized ACE2-CBD for capturing non-neutralized (infectious) RBD followed by a line of recombinant protein A for capturing neutralized RBD bound by NAb. In this LFA, a patient blood or plasma sample is diluted, briefly incubated with a polyester conjugate pad impregnated with colloidal gold-labeled RBD, and applied to the test strip. After 20 min of lateral flow across the test strip, the ratio of gold signal at the neutralized line divided by the gold signal at the infectious line (neutralized/infectious [N/I] ratio) is measured (Figure 2A) and should correlate with NAb titer. To test this, we obtained 18 serial plasma samples from one patient before and after initial mRNA vaccination with the two-dose BNT162b2 series and 16 serial plasma samples from one patient before and after the initial two-dose mRNA-1273 series. Analysis of these samples using our LFA demonstrated that the N line signal became visually apparent 2 weeks following the second dose of vaccination (Figure 2B). We quantified the signal at both the N and I lines and calculated the N/I ratio as a measure of neutralizing activity (Figures 2C and 2D; Tables S1 and S2). We observed a marked increase in the N/I ratio beginning 2 weeks after completing vaccination, followed by a decline over the course of the subsequent 4 months. We also assessed these

CellPress
OPEN ACCESS

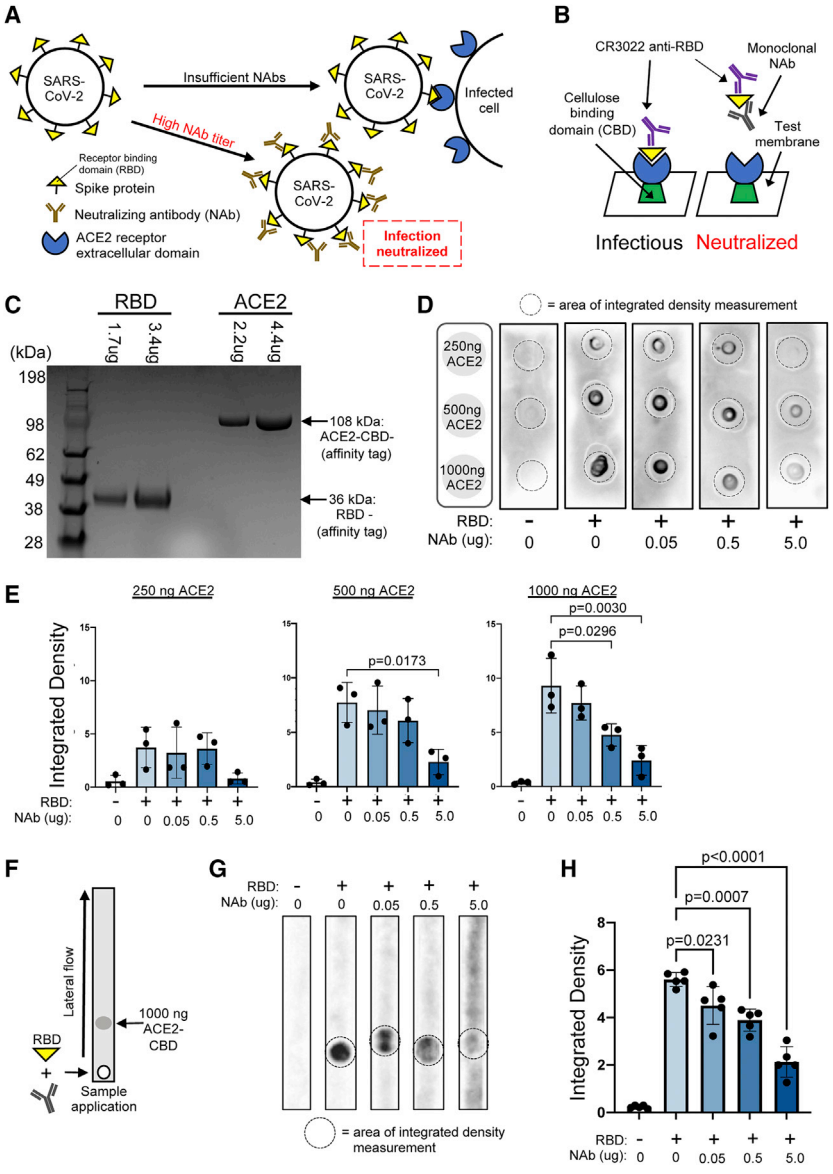

Figure 1. Membrane-based assays for detecting antibody-mediated SARS-CoV-2 neutralization

(A) Neutralizing antibodies (NAbs) can prevent SARS-CoV-2 infection by blocking the binding of the receptor-binding domain (RBD) of the viral spike protein to the ACE2 receptor on the host cell.

(B) Schematic for membrane-based dot blot assay detecting NAbs able to disrupt the binding of recombinant RBD protein to an ACE2 extracellular domain construct immobilized on a cellulose-based test membrane by protein fusion with a cellulose-binding domain (CBD). Binding of non-neutralized RBD protein to the membrane-immobilized ACE2 extracellular domain is detected by CR3022 anti-RBD monoclonal antibody followed by chemiluminescence with a horseradish peroxidase (HRP)-conjugated secondary antibody.

(C) Recombinant RBD and ACE2-CBD fusion proteins following affinity purification were analyzed by SDS-PAGE and stained with Coomassie blue. Molecular weight standards are indicated in the first lane.

(D) Monoclonal NAb inhibition of RBD binding to ACE2 in a dot blot assay. Indicated amounts of ACE2-CBD were immobilized to a cellulose membrane and incubated with RBD and indicated amounts of recombinant monoclonal SARS-CoV-2 NAb, followed by detection of RBD bound to ACE2 with CR3022 monoclonal antibody followed by HRP-conjugated secondary antibody.

(E) Quantification by background-subtracted integrated density of HRP chemiluminescent signal of RBD bound to ACE2 in dot blots, n = 3.

(F) Schematic diagram of monoclonal antibody inhibition of RBD:ACE2 binding in a lateral flow assay.

(G) RBD was mixed with indicated amounts of monoclonal NAb in pre-pandemic human plasma, applied to one end of a cellulose test strip spotted with immobilized ACE2-CBD, allowed to run via lateral flow for 15 min, and then detected with CR3022 monoclonal antibody followed by HRP-conjugated secondary antibody.

(H) Quantification by background-subtracted integrated density of HRP chemiluminescent signal of RBD bound to ACE2 in lateral flow strips, n = 5.

All error bars represent standard deviation, p values comparing indicated conditions were calculated with Student's t test.

samples with an ELISA detecting total anti-spike immunoglobulin G (IgG) antibody (Amanat et al., 2020a; Lee et al., 2020), and measured neutralization 50% inhibitory dilution (ID_{50}) titers using pseudoviral neutralization assays. The post-vaccination kinetics of neutralization ID_{50} titer were similar to the kinetics of the N/I ratio (Figures 2C and 2D; Tables S1 and S2).

To assess NAb titer following natural infection, additional plasma samples from 93 unique patients either previously infected with SARS-CoV-2 earlier than December 2020 (n = 63) or with no known exposure to SARS-CoV-2 as of December 2020 (n = 30) were obtained, analyzed with our LFA, and had anti-spike IgG and neutralization ID_{50} titers measured (Tables S1 and S2). We then evaluated the ability of our LFA to predict a range of NAb titers. For N/I ratios from 0.0 to 0.7 increasing by increments of 0.001 and anti-spike IgG levels from 0 to 2,430 mg/dL increasing by increments of 5, we calculated the sensitivity and specificity for detecting neutralization ID_{50} titers of 1:100, 1:200, 1:300, 1:500, 1:700, and 1:1,000 in the 127 total samples assessed in our study, including samples from post-vaccination and post-infection patients and patients with no known history of vaccination or infection (Table S3). Receiver operating characteristic area under the curve (ROC-AUC) analysis demonstrated that the diagnostic performance of our LFA achieved AUCs of greater than 0.85 for all titers assessed (Figure 3A). Compared with the anti-spike IgG ELISA, ROC-AUC analysis for all titers assessed in our study demonstrated a larger AUC for our LFA (Figure 3B). Since quantifying loss of RBD:ACE2 binding signal has also been proposed as a potential surrogate measure of NAb titer (Chiu et al., 2022; Huang et al., 2022; Kongsuphol et al., 2021; Lake et al.,

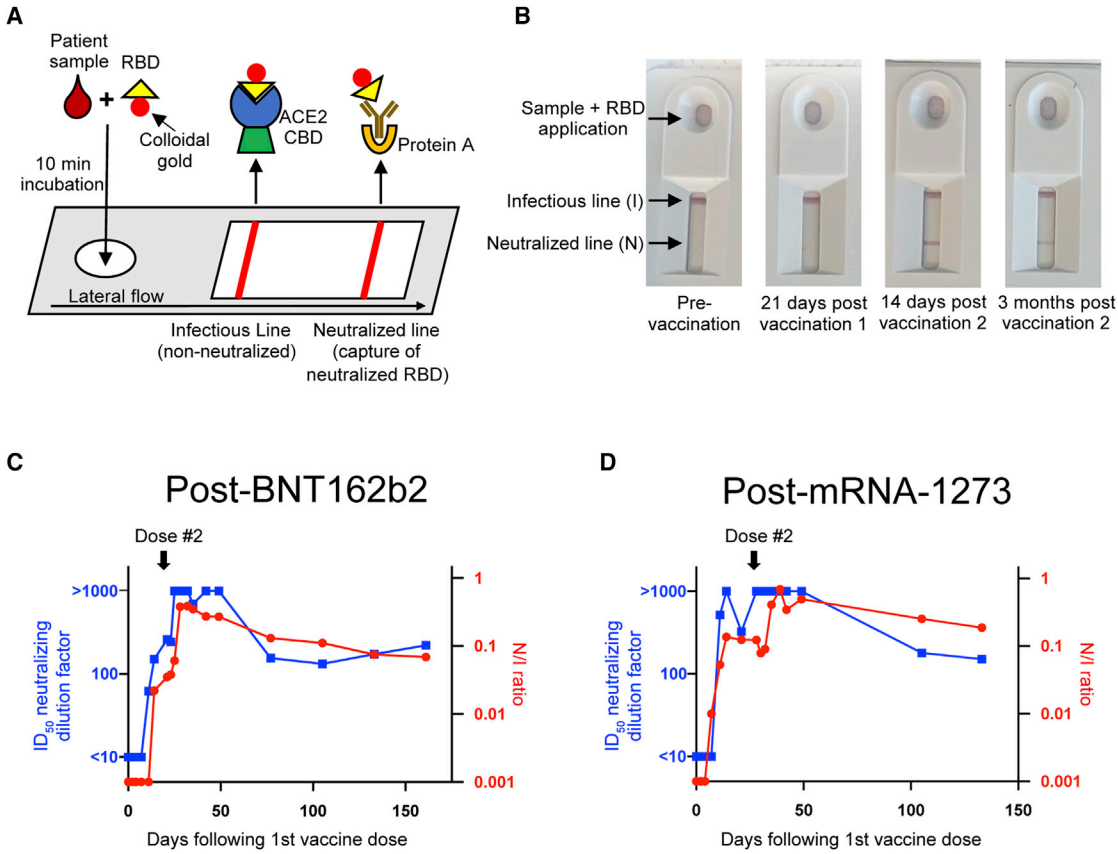

Figure 2. Lateral flow test strip performance in quantifying SARS-CoV-2 neutralizing titer in patient plasma

(A) Schematic of a rapid assay for detecting SARS-CoV-2 NAb titer in a lateral flow format. The colloidal gold-conjugated RBD protein is mixed with a patient sample and applied to one end of a membrane test strip. The infectious line contains immobilized ACE2 extracellular domain, which captures non-neutralized RBD protein, while RBD protein neutralized by NAbs migrates further to the neutralized line, where it is captured by immobilized protein A binding to the NAbs. The signal at the neutralized line divided by the signal at the infectious line (N/I ratio) determines NAb titer.

(B) Images of lateral flow neutralization test strip results for patient plasma at indicated time points following BNT162b2 vaccination.

(C and D) Time course of N/I ratio and pseudoviral neutralization ID_{50} following vaccination with either (C) BNT162b2 or (D) mRNA-1273.

2021; Wang et al., 2021), we examined the performance of this alternative approach by quantifying only loss of signal at the I line in our LFA and compared this with measuring the N/I ratio. For all six neutralization ID_{50} titers assessed, use of the N/I ratio was superior to measuring only loss of signal at the I line (Figures 3B; Table S3).

Finally, we produced a second-generation version of our LFA with greater compatibility for use in a point-of-care or at-home setting. This version has a third line (control) consisting of immobilized poly-L-lysine located distal to the I and N lines. Poly-L-lysine will capture free colloidal gold particles flowing to the end of the strip, indicating if lateral flow was successful (Figure 4A). This version also can use whole blood as the patient sample (Figure 4B). We envision that the workflow for point-of-care or at-home use would be as depicted in Figure 4C. Each test kit would contain a microcapillary tube that holds an exact volume and a finger-prick lancet (both similar to those used in certain blood glucose monitoring platforms). Each test kit would also contain a tube pre-filled with an exact volume of buffer, a polyester conjugate pad impregnated with RBD and colloidal gold, and a dropper cap to seal the tube. An exact volume of finger-prick blood (on the order of less than 10 μL) would be collected in the microcapillary tube, which would then be placed along with the impregnated pad into the buffer-filled tube. The tube would then be sealed with the dropper cap. The components would then be mixed and incubated before adding a precise number of drops onto the lateral flow strip, similar to at-home SARS-CoV-2 antigen test kits. After lateral flow for a defined time period, both qualitative and quantitative interpretation are possible. For qualitative interpretation, the cassette casing can be constructed to cover up the I line, leaving only visualization of the N and control lines, with interpretation similar to SARS-CoV-2 antigen tests: appearance of two lines indicates presence of NAbs, and appearance of only the control line indicates lack of NAbs. For quantitative interpretation, the cassette casing will allow visualization of all three lines, and a smartphone application (“app”) will use the phone’s existing camera to take a picture of the strip, quantify N and I line pixel density, and report either the calculated NAb titer or an interpretation of the level of NAb titer (e.g., none, low, moderate, high).

CellPress
OPEN ACCESS

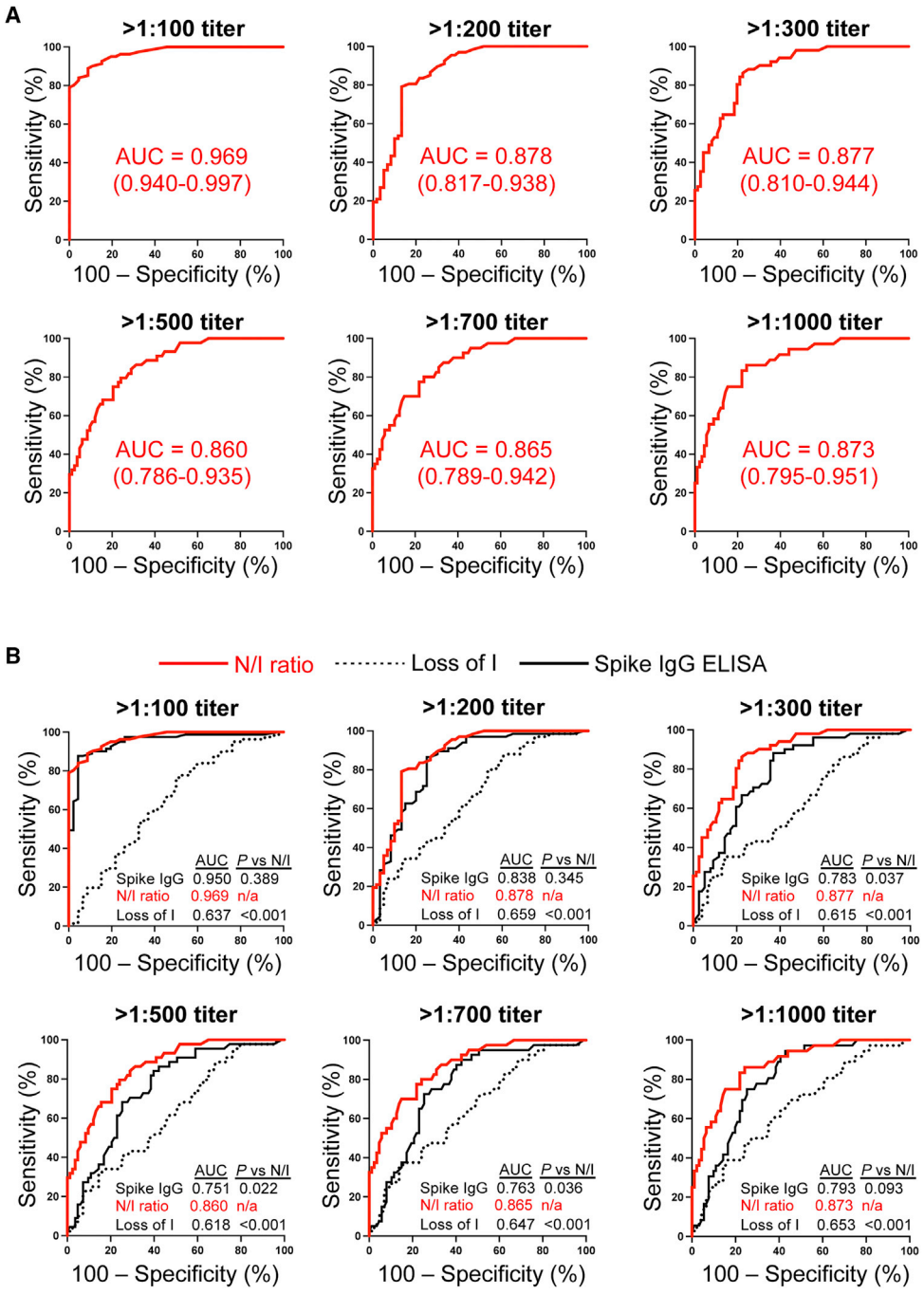

Figure 3. Lateral flow assay performance relative to alternative methodologies for assessing NAb titer

(A) Performance of LFA neutralization test strip for detecting indicated neutralization ID_{50} titers, as assessed by receiver operating characteristic area under the curve (ROS-AUC) analysis reporting sensitivity and specificity. A total of 127 plasma samples from patients previously infected with SARS-CoV-2, unvaccinated patients without known prior infection, and patients vaccinated with either BNT162b2 or mRNA-1273 were assessed. Sensitivity and specificity for detecting indicated neutralization ID_{50} titers were calculated for N/I ratios from 0 to 0.7 increasing in increments of 0.001, with sensitivity plotted versus false positive rate (100% minus specificity) to generate each ROC curve. AUC and 95% confidence interval for AUC are displayed for each titer.

(B) Comparison of diagnostic performance of N/I ratio, loss of binding signal at I line, and ELISA-based anti-spike total IgG. Sensitivity and specificity for detecting indicated neutralization ID_{50} titers were calculated for N/I ratios as in (A). I line signal integrated density from 21,000 down to 15,000 signal density units decreasing in increments of 20 and anti-spike IgG levels from 0 to 2,430 mg/dL increasing in increments of 5, with sensitivity plotted versus 100% minus specificity to generate each ROC curve. Diagnostic performance of loss of I signal and anti-spike total IgG were then calculated by ROC-AUC analysis as in (A), with p values comparing AUC with N/I ratio calculated using Pearson correlation coefficient testing.

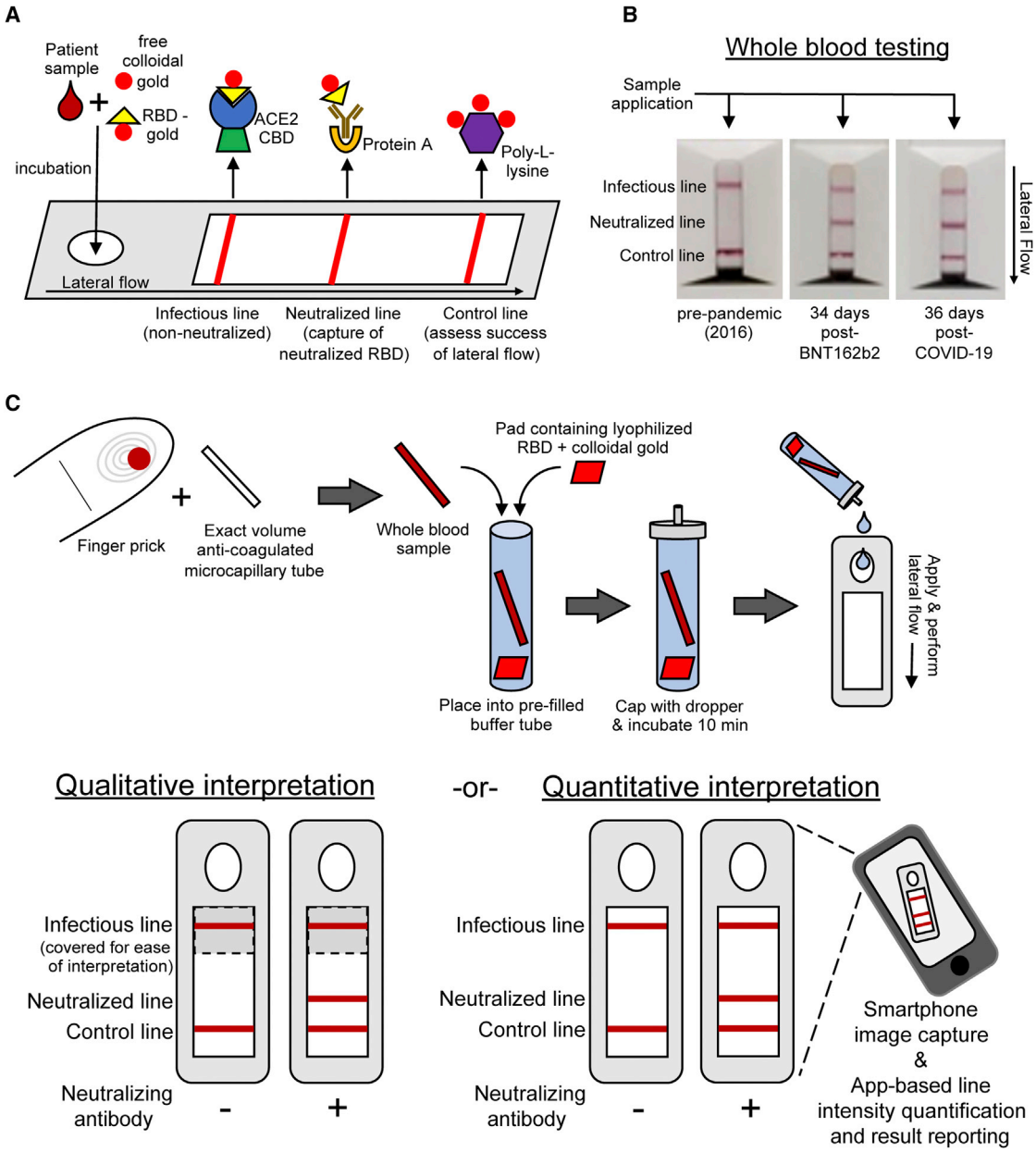

Figure 4. Lateral flow assay for at-home assessment of NAb titer

(A) Schematic of a modified lateral flow assay for detecting SARS-CoV-2 NAb titer with an additional control line to assess success of lateral flow. A mixture of colloidal gold-conjugated RBD protein and free colloidal gold is mixed with a patient sample and applied to one end of a membrane test strip. The I and N lines function similarly to Figure 2A, but a third line with immobilized poly-L-lysine captures free colloidal gold particles to indicate successful lateral flow.

(B) Images of lateral flow neutralization test strip results for patient whole-blood samples obtained either pre-pandemic, after vaccination with BNT162b2, or after recovery from COVID-19.

(C) Proposed workflow for at-home, or point-of-care, qualitative and quantitative assessment of NAb titer.

DISCUSSION

Our LFA is a tool for rapid quantification of the capability of patient plasma or blood to neutralize the RBD:ACE2 interaction. Given the diagnostic performance of our assay in predicting SARS-CoV-2 NAb titer, it has the potential to make rapid assessment of NAb titer widely available without the need for centralized laboratory processing or specialized equipment and personnel. Although our use of only the RBD portion of the SARS-CoV-2 spike protein does not assay for NAbs that neutralize spike through binding of non-RBD epitopes, we benchmarked our test against pseudoviral neutralization assays that do assess for NAbs binding to non-RBD epitopes. Thus, our approach standardizing N/I signal thresholds against

pseudoviral neutralization strives to take into account potential limitations from using RBD only. From a diagnostic methodology standpoint, our data demonstrate that for SARS-CoV-2 NAb titer, quantification of neutralized RBD with a positive signal increases test performance compared with assaying loss of RBD:ACE2 binding signal. This superior performance may be due to our developing a design in which the N line signal is normalized to the I line signal, thereby helping control for run-to-run assay variability that will undoubtedly exist in point-of-care and at-home settings. This methodology may potentially also be relevant to other infectious diseases with well-characterized epitopes for binding to surface receptors.

As our LFA platform is compatible with existing optical capture of signal intensity using smartphone technology (Parker et al., 2020; Urusov et al., 2019; Wood et al., 2019), creation of a smartphone "app" specific to the final version of our assay would allow quantitative interpretation at the point of care or in the at-home setting. Additionally, because this LFA platform incorporates a recombinant RBD protein that can be modularly substituted for the RBD of a SARS-CoV-2 spike protein variant of interest (VOI), our assay should be adaptable to VOIs so long as the RBD or spike protein of the variant can be quickly produced at scale in a recombinant fashion (Argentinian AntiCovid, 2020; Dalvie et al., 2021; Pino et al., 2021; Pollet et al., 2021; Zang et al., 2021). Future studies determining NAb signal in our LFA following infection with SARS-CoV-2 VOIs will be important, as new variants are likely to continue appearing, but orthogonal studies identifying what neutralization titers against the original SARS-CoV-2 strain are required to protect against VOIs will also be helpful in this regard (Ai et al., 2022; Evans et al., 2022a, 2022b). Finally, as this LFA reports a quantitative assessment of NAb titer, we believe it will be useful as a cost-effective (Figure S1B), easily distributable assay in large-scale studies to define the degree of RBD:ACE2 interaction inhibition that correlates with protection from SARS-CoV-2 infection. A consensus in the field is currently lacking for this significant question regarding SARS-CoV-2 immune responses (Krammer, 2021). Once protective titers have been defined, this LFA and others (Duan et al., 2022; Fulford et al., 2021; Wang et al., 2022) could contribute to population-scale serial monitoring efforts to determine the time point at which individuals in the general population, or high-risk occupations, lose protective immunity and benefit from repeat vaccination.

Limitations of the study

The method for quantifying SARS-CoV-2 NAbs titer at the point of care that we developed uses neutralization of RBD binding to ACE2 as a surrogate measurement. This methodology will not detect NAbs that have a neutralization mechanism of action that is independent of blocking RBD binding to ACE2. The prototype we generated assays the ability of NAbs to block RBD from the original strain of SARS-CoV-2 from binding to ACE2, and the convalescent plasma we used to validate our method was only collected from patients likely infected with the original strain given the timing of when convalescent plasma samples were collected. Although this methodology can be adapted to the continuously arising spike protein variants, the approach may have to be validated for current and future spike protein variants.

STAR★METHODS

Detailed methods are provided in the online version of this paper and include the following:

- KEY RESOURCES TABLE
- RESOURCE AVAILABILITY
  - Lead contact
  - Materials availability
  - Data and code availability
- EXPERIMENTAL MODEL AND SUBJECT DETAILS
  - Cell lines
  - Human samples
- METHOD DETAILS
  - Generation of stable cell lines
  - Purification of recombinant proteins
  - Dot blot assessment of RBD-ACE2 interaction
  - Pilot lateral flow assessment of RBD-ACE2 interaction
  - Lateral flow assay cassette construction
  - Human sample processing
  - Lateral flow assay protocol
  - Pseudoviral neutralization assay
  - Anti-spike IgG ELISA
- QUANTIFICATION AND STATISTICAL ANALYSIS
  - Sensitivity and specificity calculations
  - Receiver operating characteristic (ROC) curve generation
- STATISTICAL ANALYSIS FOR COMPARING TWO ROC CURVES

SUPPLEMENTAL INFORMATION

Supplemental information can be found online at https://doi.org/10.1016/j.crmeth.2022.100273.

ACKNOWLEDGMENTS

The authors would like to thank Gail Bell, Tatum Braun, Christopher Nabel, Sharon Onggo, and Katherine Waters for technical assistance and Salil Garg for helpful discussion. This work was supported in part by the Koch Institute Support Core grant P30-CA14051 from the National Cancer Institute. We thank the Koch Institute's Robert A. Swanson (1969) Biotechnology Center for technical support, specifically the Flow Cytometry Core. H.L. is supported by the Charles W. (1955) and Jennifer C. Johnson Cancer Research Fund, an American Society of Hematology Scholar award, and a National Institutes of Health grant K08-DK123414. D.C.L. and M.B.Y. are supported in part by the Charles and Marjorie Holloway Foundation.

AUTHOR CONTRIBUTIONS

G.G.C., O.O.K., S.B., D.C.L., R.M.W., E.J.R., D.M.T., L.H., A.C., C.M.-A., E.K.W.T., M.B.Y., R.C.B., H.D.S., and H.L. designed the research, reagents, and prototype. G.G.C., O.O.K., S.B., D.C.L., R.M.W., E.J.R., H.J., R.D.H., N.K.H., W.B.L., P.Y.L., F.K., R.C.B., and H.L. generated the reagents and prototype, performed the research, and analyzed the data. A.N.K., M.B.Y., P.Y.L., R.C.B., S.N.B., H.D.S., and H.L. supervised the work and obtained funding. All authors contributed to writing and editing the manuscript.

DECLARATION OF INTERESTS

S.B. and R.C.B. were employees of Cataloid Products when this work was performed. As of December 1, 2020, E.J.R. is an employee of Dragonfly

Therapeutics. As of February 1, 2021, A.C. is an employee of Satellite Bio. The Massachusetts Institute of Technology has filed patents related to this technology on behalf of G.G.C. and H.L. The Icahn School of Medicine at Mount Sinai has filed patent applications relating to SARS-CoV-2 serological assays and NDV-based SARS-CoV-2 vaccines, which list F.K. as co-inventor. Mount Sinai has spun out a company, Kantaro, to market serological tests for SARS-CoV-2. F.K. has consulted for Merck and Pfizer (before 2020) and is currently consulting for Pfizer, Third Rock Ventures, Seqirus, and Avimex. The F.K. laboratory is also collaborating with Pfizer on animal models of SARS-CoV-2. As of August 23, 2021, G.G.C. is affiliated with Duke University. As of July 1, 2022, R.D.H. is affiliated with University of Arizona College of Medicine at Tucson. As of August 31, 2021, H.J. is affiliated with Dartmouth University.

Received: February 3, 2022
Revised: June 13, 2022
Accepted: July 22, 2022
Published: August 4, 2022

REFERENCES

Ai, J., Wang, X., He, X., Zhao, X., Zhang, Y., Jiang, Y., Li, M., Cui, Y., Chen, Y., Qiao, R., et al. (2022). Antibody evasion of SARS-CoV-2 Omicron BA.1, BA.1.1, BA.2, and BA.3 sub-lineages. Cell Host Microbe.

Amanat, F., Stadlbauer, D., Strohmeier, S., Nguyen, T.H.O., Chromikova, V., McMahon, M., Jiang, K., Arunkumar, G.A., Jurczyszak, D., Polanco, J., et al. (2020a). A serological assay to detect SARS-CoV-2 seroconversion in humans. Nat. Med. *26*, 1033–1036.

Amanat, F., White, K.M., Miorin, L., Strohmeier, S., McMahon, M., Meade, P., Liu, W.C., Albrecht, R.A., Simon, V., Martinez-Sobrido, L., et al. (2020b). An in vitro microneutralization assay for SARS-CoV-2 serology and drug screening. Curr. Protoc. Microbiol. *58*, e108.

Argentinian AntiCovid Consortium (2020). Structural and functional comparison of SARS-CoV-2-spike receptor binding domain produced in Pichia pastoris and mammalian cells. Sci. Rep. *10*, 21779.

Bewley, K.R., Coombes, N.S., Gagnon, L., McInroy, L., Baker, N., Shaik, I., St-Jean, J.R., St-Amant, N., Buttigieg, K.R., Humphries, H.E., et al. (2021). Quantification of SARS-CoV-2 neutralizing antibody by wild-type plaque reduction neutralization, microneutralization and pseudotyped virus neutralization assays. Nat. Protoc. *16*, 3114–3140.

Chiu, W.H., Kong, W.Y., Su, Y.J., Wen, J.W., Tsai, C.M., Hong, C., Chen, P.Y., and Ko, C.H. (2022). A faster, novel technique to detect COVID-19 neutralizing antibodies. Med. Sci. Mon. Int. Med. J. Exp. Clin. Res. *28*, e935812.

Collier, A.R.Y., Yu, J., McMahan, K., Liu, J., Chandrashekar, A., Maron, J.S., Atyeo, C., Martinez, D.R., Ansel, J.L., Aguayo, R., et al. (2021). Differential kinetics of immune responses elicited by covid-19 vaccines. N. Engl. J. Med. *385*, 2010–2012.

Crawford, K.H.D., Eguia, R., Dingens, A.S., Loes, A.N., Malone, K.D., Wolf, C.R., Chu, H.Y., Tortorici, M.A., Veesler, D., Murphy, M., et al. (2020). Protocol and reagents for pseudotyping lentiviral particles with SARS-CoV-2 spike protein for neutralization assays. Viruses *12*.

Dalvie, N.C., Rodriguez-Aponte, S.A., Hartwell, B.L., Tostanoski, L.H., Biedermann, A.M., Crowell, L.E., Kaur, K., Kumru, O.S., Carter, L., Yu, J., et al. (2021). Engineered SARS-CoV-2 receptor binding domain improves manufacturability in yeast and immunogenicity in mice. Proc. Natl. Acad. Sci. USA *118*. e2106845118.

Duan, X., Shi, Y., Zhang, X., Ge, X., Fan, R., Guo, J., Li, Y., Li, G., Ding, Y., Osman, R.A., et al. (2022). Dual-detection fluorescent immunochromatographic assay for quantitative detection of SARS-CoV-2 spike RBD-ACE2 blocking neutralizing antibody. Biosens. Bioelectron. *199*, 113883.

Evans, J.P., Qu, P., Zeng, C., Zheng, Y.M., Carlin, C., Bednash, J.S., Lozanski, G., Mallampalli, R.K., Saif, L.J., Oltz, E.M., et al. (2022a). Neutralization of the SARS-CoV-2 deltacron and BA.3 variants. N. Engl. J. Med. *386*, 2340–2342.

Evans, J.P., Zeng, C., Qu, P., Faraone, J., Zheng, Y.M., Carlin, C., Bednash, J.S., Zhou, T., Lozanski, G., Mallampalli, R., et al. (2022b). Neutralization of SARS-CoV-2 omicron sub-lineages BA.1, BA.1.1, and BA.2. Cell Host Microbe.

Even, D.Y., Kedmi, A., Basch-Barzilay, S., Ideses, D., Tikotzki, R., Shir-Shapira, H., Shefi, O., and Juven-Gershon, T. (2016). Engineered promoters for potent transient overexpression. PLoS One *11*, e0148918.

Fulford, T.S., Van, H., Gherardin, N.A., Zheng, S., Ciula, M., Drummer, H.E., Redmond, S., Tan, H.X., Boo, I., Center, R.J., et al. (2021). A point-of-care lateral flow assay for neutralising antibodies against SARS-CoV-2. EBioMedicine *74*, 103729.

Gibson, D.G., Young, L., Chuang, R.Y., Venter, J.C., Hutchison, C.A., 3rd, and Smith, H.O. (2009). Enzymatic assembly of DNA molecules up to several hundred kilobases. Nat. Methods *6*, 343–345.

Gilbert, P.B., Montefiori, D.C., McDermott, A.B., Fong, Y., Benkeser, D., Deng, W., Zhou, H., Houchens, C.R., Martins, K., Jayashankar, L., et al. (2022). Immune correlates analysis of the mRNA-1273 COVID-19 vaccine efficacy clinical trial. Science *375*, 43–50.

Goldberg, Y., Mandel, M., Bar-On, Y.M., Bodenheimer, O., Freedman, L., Haas, E.J., Milo, R., Alroy-Preis, S., Ash, N., and Huppert, A. (2021). Waning immunity after the BNT162b2 vaccine in Israel. N. Engl. J. Med. *385*, e85.

Götzke, H., Kilisch, M., Martínez-Carranza, M., Sograte-Idrissi, S., Rajavel, A., Schlichthaerle, T., Engels, N., Jungmann, R., Stenmark, P., Opazo, F., and Frey, S. (2019). The ALFA-tag is a highly versatile tool for nanobody-based bioscience applications. Nat. Commun. *10*, 4403.

Hanley, J.A., and McNeil, B.J. (1983). A method of comparing the areas under receiver operating characteristic curves derived from the same cases. Radiology *148*, 839–843.

Huang, R.L., Fu, Y.C., Wang, Y.C., Hong, C., Yang, W.C., Wang, I.J., Sun, J.R., Chen, Y., Shen, C.F., and Cheng, C.M. (2022). A lateral flow immunoassay coupled with a spectrum-based reader for SARS-CoV-2 neutralizing antibody detection. Vaccines (Basel) *10*.

Huo, J., Zhao, Y., Ren, J., Zhou, D., Duyvesteyn, H.M.E., Ginn, H.M., Carrique, L., Malinauskas, T., Ruza, R.R., Shah, P.N.M., et al. (2020). Neutralization of SARS-CoV-2 by destruction of the prefusion spike. Cell Host Microbe *28*, 445–454.e46.

Khoury, D.S., Cromer, D., Reynaldi, A., Schlub, T.E., Wheatley, A.K., Juno, J.A., Subbarao, K., Kent, S.J., Triccas, J.A., and Davenport, M.P. (2021). Neutralizing antibody levels are highly predictive of immune protection from symptomatic SARS-CoV-2 infection. Nat. Med. *27*, 1205–1211.

Kongsuphol, P., Jia, H., Cheng, H.L., Gu, Y., Shunmuganathan, B.D., Chen, M.W., Lim, S.M., Ng, S.Y., Tambyah, P.A., Nasir, H., et al. (2021). A rapid simple point-of-care assay for the detection of SARS-CoV-2 neutralizing antibodies. Commun. Med. *1*, 1–12.

Krammer, F. (2021). A correlate of protection for SARS-CoV-2 vaccines is urgently needed. Nat. Med. *27*, 1147–1148.

Lake, D.F., Roeder, A.J., Kaleta, E., Jasbi, P., Pfeffer, K., Koelbela, C., Periasamy, S., Kuzmina, N., Bukreyev, A., Grys, T.E., et al. (2021). Development of a rapid point-of-care test that measures neutralizing antibodies to SARS-CoV-2. J. Clin. Virol. *145*, 105024.

Lee, P.Y., Day-Lewis, M., Henderson, L.A., Friedman, K.G., Lo, J., Roberts, J.E., Lo, M.S., Platt, C.D., Chou, J., Hoyt, K.J., et al. (2020). Distinct clinical and immunological features of SARS-CoV-2-induced multisystem inflammatory syndrome in children. J. Clin. Invest. *130*, 5942–5950.

Letko, M., Marzi, A., and Munster, V. (2020). Functional assessment of cell entry and receptor usage for SARS-CoV-2 and other lineage B betacoronaviruses. Nat. Microbiol. *5*, 562–569.

Lisboa Bastos, M., Tavaziva, G., Abidi, S.K., Campbell, J.R., Haraoui, L.P., Johnston, J.C., Lan, Z., Law, S., MacLean, E., Trajman, A., et al. (2020). Diagnostic accuracy of serological tests for covid-19: systematic review and meta-analysis. BMJ *370*, m2516.

Manenti, A., Maggetti, M., Casa, E., Martinuzzi, D., Torelli, A., Trombetta, C.M., Marchi, S., and Montomoli, E. (2020). Evaluation of SARS-CoV-2 neutralizing antibodies using a CPE-based colorimetric live virus micro-neutralization assay in human serum samples. J. Med. Virol. *92*, 2096–2104.

Miller, E.A., Baniya, S., Osorio, D., Al Maalouf, Y.J., and Sikes, H.D. (2018). Paper-based diagnostics in the antigen-depletion regime: high-density immobilization of rcSso7d-cellulose-binding domain fusion proteins for efficient target capture. Biosens. Bioelectron. *102*, 456–463.

Müller-Kuller, U., Ackermann, M., Kolodziej, S., Brendel, C., Fritsch, J., Lachmann, N., Kunkel, H., Lausen, J., Schambach, A., Moritz, T., and Grez, M. (2015). A minimal ubiquitous chromatin opening element (UCOE) effectively prevents silencing of juxtaposed heterologous promoters by epigenetic remodeling in multipotent and pluripotent stem cells. Nucleic Acids Res. *43*, 1577–1592.

Murphy, G.J., Mostoslavsky, G., Kotton, D.N., and Mulligan, R.C. (2006). Exogenous control of mammalian gene expression via modulation of translational termination. Nat. Med. *12*, 1093–1099.

Murray, L.P., and Mace, C.R. (2020). Usability as a guiding principle for the design of paper-based, point-of-care devices - a review. Anal. Chim. Acta *1140*, 236–249.

Nandakumar, V., Profaizer, T., Lozier, B.K., Elgort, M.G., Larragoite, E.T., Williams, E.S.C.P., Solis-Leal, A., Lopez, J.B., Berges, B.K., Planelles, V., et al. (2021). Evaluation of a surrogate enzyme-linked immunosorbent assay-based severe acute respiratory syndrome coronavirus 2 (SARS-CoV-2) cPass neutralization antibody detection assay and correlation with immunoglobulin G commercial serology assays. Arch. Pathol. Lab Med. *145*, 1212–1220.

Nie, J., Li, Q., Wu, J., Zhao, C., Hao, H., Liu, H., Zhang, L., Nie, L., Qin, H., Wang, M., et al. (2020). Establishment and validation of a pseudovirus neutralization assay for SARS-CoV-2. Emerg. Microb. Infect. *9*, 680–686.

Parker, R.W., Wilson, D.J., and Mace, C.R. (2020). Open software platform for automated analysis of paper-based microfluidic devices. Sci. Rep. *10*, 11284.

Pino, M., Abid, T., Pereira Ribeiro, S., Edara, V.V., Floyd, K., Smith, J.C., Latif, M.B., Pacheco-Sanchez, G., Dutta, D., Wang, S., et al. (2021). A yeast expressed RBD-based SARS-CoV-2 vaccine formulated with 3M-052-alum adjuvant promotes protective efficacy in non-human primates. Sci. Immunol. *6*, eabh3634.

Pollet, J., Chen, W.H., Versteeg, L., Keegan, B., Zhan, B., Wei, J., Liu, Z., Lee, J., Kundu, R., Adhikari, R., et al. (2021). SARSCoV-2 RBD219-N1C1: a yeast-expressed SARS-CoV-2 recombinant receptor-binding domain candidate vaccine stimulates virus neutralizing antibodies and T-cell immunity in mice. Hum. Vaccines Immunother. *17*, 2356–2366.

Tan, C.W., Chia, W.N., Qin, X., Liu, P., Chen, M.I.C., Tiu, C., Hu, Z., Chen, V.C.W., Young, B.E., Sia, W.R., et al. (2020). A SARS-CoV-2 surrogate virus neutralization test based on antibody-mediated blockage of ACE2-spike protein-protein interaction. Nat. Biotechnol. *38*, 1073–1078.

Tanenbaum, M.E., Gilbert, L.A., Qi, L.S., Weissman, J.S., and Vale, R.D. (2014). A protein-tagging system for signal amplification in gene expression and fluorescence imaging. Cell *159*, 635–646.

ter Meulen, J., van den Brink, E.N., Poon, L.L.M., Marissen, W.E., Leung, C.S.W., Cox, F., Cheung, C.Y., Bakker, A.Q., Bogaards, J.A., van Deventer, E., et al. (2006). Human monoclonal antibody combination against SARS coronavirus: synergy and coverage of escape mutants. PLoS Med. *3*, e237.

Urusov, A.E., Zherdev, A.V., and Dzantiev, B.B. (2019). Towards lateral flow quantitative assays: detection approaches. Biosensors *9*, E89.

Wang, J.J., Zhang, N., Richardson, S.A., and Wu, J.V. (2021). Rapid lateral flow tests for the detection of SARS-CoV-2 neutralizing antibodies. Expert Rev. Mol. Diagn. *21*, 363–370.

Wang, Q., Feng, L., Zhang, H., Gao, J., Mao, C., Landesman-Bollag, E., Mostoslavsky, G., Lunderberg, J.M., Zheng, W., Hao, S., and Gao, W. (2022). Longitudinal waning of mRNA vaccine-induced neutralizing antibodies against SARS-CoV-2 detected by an LFIA rapid test. Antib. Ther. *5*, 55–62.

Wood, C.S., Thomas, M.R., Budd, J., Mashamba-Thompson, T.P., Herbst, K., Pillay, D., Peeling, R.W., Johnson, A.M., McKendry, R.A., and Stevens, M.M. (2019). Taking connected mobile-health diagnostics of infectious diseases to the field. Nature *566*, 467–474.

Wrapp, D., Wang, N., Corbett, K.S., Goldsmith, J.A., Hsieh, C.L., Abiona, O., Graham, B.S., and McLellan, J.S. (2020). Cryo-EM structure of the 2019-nCoV spike in the prefusion conformation. Science *367*, 1260–1263.

Yan, R., Zhang, Y., Li, Y., Xia, L., Guo, Y., and Zhou, Q. (2020). Structural basis for the recognition of SARS-CoV-2 by full-length human ACE2. Science *367*, 1444–1448.

Yun, S., Ryu, J.H., Jang, J.H., Bae, H., Yoo, S.H., Choi, A.R., Jo, S.J., Lim, J., Lee, J., Ryu, H., et al. (2021). Comparison of SARS-CoV-2 antibody responses and seroconversion in COVID-19 patients using twelve commercial immunoassays. Ann. Lab. Med. *41*, 577–587.

Zang, J., Zhu, Y., Zhou, Y., Gu, C., Yi, Y., Wang, S., Xu, S., Hu, G., Du, S., Yin, Y., et al. (2021). Yeast-produced RBD-based recombinant protein vaccines elicit broadly neutralizing antibodies and durable protective immunity against SARS-CoV-2 infection. Cell Discov. *7*, 71.

STAR★METHODS

KEY RESOURCES TABLE

REAGENT or RESOURCE	SOURCE	IDENTIFIER
Antibodies		
SARS-CoV-2 Neutralizing Antibody	ABclonal	Cat# A19215; RRID: AB_2862633
Anti-COVID-19 & SARS-CoV S glycoprotein [CR3022]	Absolute Antibody	Cat# Ab01680-3.3; RRID: AB_2848080
Anti-Mouse IgG HRP-linked	Cell Signaling	Cat# 7076; RRID: AB_1001768
Goat Anti-Human IgG-HRP	Southern Biotech	Cat# 2040-05; RRID: AB_2795644
Purified anti-SARS-CoV-2 S Protein S1 Recombinant Antibody	Biolegend	Cat# 938701; RRID: AB_2876764
Bacterial and virus strains		
Spike (SARS-CoV-2) Pseudotyped Lentivirus (Luciferase Reporter)	BPS Bioscience	Cat# 79942
Biological samples		
Human Peripheral Blood Plasma, Frozen	Stem Cell Technologies	Cat# 70039.6
SARS-CoV-2 Positive CL	BioIVT	N/A
COVID-19 Plasma Sample Set	Ray Biotech	Cat# CoV-PosSet-S1; CoV-PosSet-S2; CoV-PosSet-S3
Human Peripheral Blood Plasma post-BNT-162b2 vaccination	Boston Children's Hospital IRB-approved protocol	N/A
Human Peripheral Blood Plasma post-mRNA-1273 vaccination	Boston Children's Hospital IRB-approved protocol	N/A
Chemicals, peptides, and recombinant proteins		
Recombinant SARS-CoV-2 S-RBD	Generated by the authors for this manuscript	N/A
Recombinant ACE-2 CBD	Generated by the authors for this manuscript	N/A
Recombinant Protein A	Sinobiological	Cat# 10600-P07E
Recombinant SARS-CoV-2 S Protein S1	Biolegend	Cat# 792904
Strep-Tactin Sepharose 50% Suspension	Neuromics Antibodies	Cat# 2-1201-010
Bovine Serum Albumin	Millipore Sigma	Cat# A8531
Blasticidin S HCl, powder	Thermo Fisher Scientific	Cat# R21001
Poly-L-lysine	Millipore Sigma	Cat# P3513
Coomassie Brilliant Blue R-250 Dye	Thermo Fisher Scientific	Cat# 20278
TWEEN® 20	Milllipore Sigma	Cat# P9416
Critical commercial assays		
NEBuilder® HiFi DNA Assembly Cloning Kit	New England Biolabs	Cat# E5520S
ONE-Step™ Luciferase Assay System	BPS Bioscience	Cat# 60690
CalPhos™ Mammalian Transfection Kit	Clontech Laboratories	Cat# 631312
Pierce™ ECL Western Blotting Substrate	Thermo Fisher Scientific	Cat# 32106
TMB Substrate Set	Biolegend	Cat# 421101
Experimental models: Cell lines		
ACE2 expressing HEK293 cells	BPS Bioscience	Cat# 79951
HEK293T Stable RBD Expression Cell Line	This paper	N/A
HEK293T Stabe ACE2 Expression Cell Line	This paper	N/A
293T	ATCC	Cat# CRL-3216™

(*Continued on next page*)

Continued

REAGENT or RESOURCE	SOURCE	IDENTIFIER
Software and algorithms		
ImageJ	NIH	https://imagej.nih.gov/ij/
GraphPad Prism 8.0	GraphPad Software	https://www.graphpad.com/
NCSS Statistical Software	NCSS	https://www.ncss.com/
Other		
Growth Medium 1N	BPS Bioscience	Cat# 79801
Nunc-Immuno™ MicroWell™ 96 well solid plates	Millipore Sigma	Cat# M9410
Model G2 Gyrotory Shaker	New Brunswick Scientific Co.	N/A
Fujifilm X-E2S digital camera	Fujifilm	N/A
Galaxy S9	Samsung	N/A
iPhone X	Apple	N/A
Infinite M200 PRO Plate Reader	Tecan	N/A
Lohmann GL-422 clear cover-stock	Lohmann Technologies	N/A
Synergy HTX Reader	BioTek	N/A
LFA Running Buffer	Catalloid Products, Inc.	Cat# NAB-RB2
Ahlstrom 8964 fiber glass sample pad	Ahlstrom-Munksjo	N/A
Sartorius CN95 nitrocellulose membrane	Sartorius	N/A
Ahlstrom 222 absorbent pad	Ahlstrom-Munksjo	N/A
RBD Colloidal Gold Pad	This paper	N/A
Whatman® cellulose chromatography papers	Millipore Sigma	Cat# WHA3001845
Amicon® Ultra-4 Centrifugal Filter Unit	Millipore Sigma	Cat# UFC810024

RESOURCE AVAILABILITY

Lead contact

Further information and requests for resources and reagents should be directed to and will be fulfilled by the lead contact, Hojun Li (hojunli@mit.edu).

Materials availability

All non-commercially available materials generated in this study can be requested by contacting the lead contact (H.L.), including lentiviral vector plasmids for ACE2 and RBD and stable HEK293T producer cell lines for recombinant ACE2 and recombinant RBD.

Data and code availability

- All data generated in this study are available in the main figures and supplemental tables.
- This paper does not report original code.
- Any additional information required to reanalyze the data reported in this paper is available from the lead contact upon request.

EXPERIMENTAL MODEL AND SUBJECT DETAILS

Cell lines

293T cells were obtained from American Type Culture Collection (ATCC). Both prior to lentiviral transduction and after lentiviral transduction for recombinant protein production, 293T cells were maintained in Dulbecco's Modified Eagle Medium (ATCC) supplemented with 10% fetal bovine serum (CPS serum) and penicillin/streptomycin (Gibco) in a humidified incubator at 37°C with 5% CO_2. 293T cells were thawed directly after receipt from ATCC, and were authenticated by ATCC with STR profiling. The sex of 293T cells is not provided by ATCC.

Human samples

Post-vaccination human blood samples from a 24-year-old-male and a 36-year-old-male were collected in accordance with a protocol approved by the Boston Children's Hospital Institutional Review Board. De-identified blood and plasma samples collected prior

to December 2020 from human subjects previously infected with SARS-CoV-2, or with no known previous SARS-CoV-2 exposure, were purchased from commercial vendors BioIVT and Ray Biotech. Human samples were handled in accordance with biosafety protocols in compliance with regulations of Boston Children's Hospital. Samples sizes are detailed in the Results section and Figure Legends of the manuscript.

METHOD DETAILS

Generation of stable cell lines

Lentiviral constructs for creation of stable cell lines expressing the RBD and ACE2 ectodomain constructs were created using a pHAGE2-based vector (Murphy et al., 2006) for constitutive expression of the transgene using a cytomegalovirus (CMV) promoter flanked by a mini ubiquitous chromatin opening element (miniUCOE) (Muller-Kuller et al., 2015) and a super core promoter 3 (SCP3) elements (Even et al., 2016). The vector also incorporates an IRES-blasticidin S deaminase-T2A-EGFP cassette downstream of the transgene for selection using blasticidin and fluorescence activated cell sorting (FACS) based on EGFP expression level. Constructs were assembled using Gibson Assembly (Gibson et al., 2009) with the NEBuilder HiFi DNA assembly kit (New England Biolabs). A lentiviral construct for an RBD construct C-terminally tagged with His8, FLAG, StrepTag2, ALFA (Gotzke et al., 2019), and GCN4 (Tanenbaum et al., 2014) tags was assembled from the RBD sequence PCR amplified from pCAGGS-spikeRBD, while the sequences for the C-terminal tags were PCR amplified from gBlocks (Integrated DNA Technologies) codon optimized for expression in human cells. A lentiviral construct for the ACE2 ectodomain (residues 1-739) C-terminally tagged with His8, FLAG, StrepTag2 and cellulose binding domain (CBD) was assembled from fragments PCR amplified from codon-optimized gBlocks (Integrated DNA technologies).

Lentiviruses were produced in 293T cells, by calcium phosphate co-transfection (CalPhos mammalian transfection kit, Clontech Laboratories) of packaging vectors (pCMV-VSV-G envelope and pCMV-dR8.2 dvpr) together with either the RBD- or ACE2 ectodomain-expressing lentiviral construct. Virus-containing media were filtered through 0.45 μm filters and used to transduce 293T cells. Stably transduced cells were selected with 10 μg/mL Blasticidin (Promega) and sorted for cells with high levels of protein expression by FACS using the EGFP expression level as a proxy for expression of the transgene.

Purification of recombinant proteins

Media supernatant was collected from the stable cell lines every other day for two weeks. The supernatant was stored at 4°C until the end of the two-week period when it was then centrifuged at 700 × g for 5 min to clear any cellular debris. The spun down supernatant was then sterile filtered using a 0.2 μm filter into a sterile bottle. Using an ÄKTA start system, a column filled with 1mL of sedimented Strep-Tactin (Neuromics Antibodies) resin was attached and washed with 15 mL of 50 mM 4-(2-hydroxyethyl)-1-piperazineethanesulfonic acid (HEPES) buffer. The media supernatant was run through the column at a speed of 1 mL/min overnight at 4°C. The column was washed for 15 min with 15 mL of wash buffer (50 mM HEPES) and was then switched out for elution buffer (50mM biotin HEPES). Elution buffer was run through the column until the UV absorbance returned to the level it was prior to elution. The elution product was then concentrated via a 100,000 kDa molecular weight cut-off centrifuge tubes (Millipore Sigma). Concentration was then measured by bicinchoninic acid (BCA) assay analysis. Purity was analyzed by running 2 μL & 5 μL of elute product on a sodium dodecyl sulphate–polyacrylamide gel electrophoresis (SDS-PAGE) gel, then stained with Coomassie blue (ThermoFisher Scientific).

Dot blot assessment of RBD-ACE2 interaction

Serial dilutions of the recombinant ACE2-CBD were made in the same buffer it was eluted in to yield 250, 500, and 1000 ng of ACE2-CBD per 3 μL of solution. The serial dilutions were applied to cellulose membrane (Whatman #2, Millipore Sigma) cut to size and incubated at 37°C for 2 h. The membranes were then blocked in 3% bovine serum albumin (BSA, Sigma) for 1 h at 25°C. Primary incubation solutions were made in 3% BSA buffer with RBD at a concentration of 1 μg/mL (except for the no RBD condition) and increasing NAb amounts (0.05, 0.5, and 5 μg NAb); all solutions had a final volume of 1 mL. The NAb used was a SARS-CoV-2 Neutralizing Antibody (ABclonal). The primary incubation solutions were all incubated on ice for 15 min. Blocking buffer was discarded, primary solution was added and set to incubate at 4°C for 1 h. Blots were then washed 3 times for 5 min each with Tris-buffered saline with 0.1% Tween-20 (TBST) buffer (Millipore Sigma). Primary antibody (Mouse IgG2A-modified Anti-COVID-19 & SARS-CoV S glycoprotein [CR3022 (ter Meulen et al., 2006)], Absolute Antibody) solution was applied at a 1:1000 dilution in TBST buffer and incubated at 4°C overnight. Blots were washed again with TBST, 3 times for 5 min each. Next, anti-mouse IgG- horseradish peroxidase conjugated secondary antibody (Cell Signaling Technologies) was diluted into 3% BSA TBST buffer at 1:5000, applied to blots and incubated at 25°C for 1 h. Membranes were then washed again with TBST, 3 times, 5 min each. Enhanced chemiluminescence (ECL) reagent (ThermoFisher) was mixed and applied to each blot for 5 min, then blotted off. Blots were then all exposed and imaged together via a Bio-Rad ChemiDoc XRS+ system on auto-exposure. Images were saved in .tiff format. Integrated density analysis of dot blots was performed using ImageJ software according to the ImageJ NIH Dot Blot Analysis tutorial. In brief, the .tiff format images were uploaded to ImageJ and background subtracted with a rolling ball radius set to 33 pixels. Images were then inverted

in order to ensure background pixels would be equal to nearly zero. A circular selection lasso was made and moved over each measurement area to collect the integrated density values. The output of the measurement was the sum of all pixels in the circular selection.

Pilot lateral flow assessment of RBD-ACE2 interaction

Whatman #2 cellulose membrane was cut it into thin strips of 0.5 cm by 8.5 cm. At 2 cm up from the bottom of the strip, 1 μg of ACE2-CBD was applied and the strips were then dried at 37°C for 2 h. The strips were then blocked with 3% BSA TBST solution for 1 h at 25°C. Afterwards, the strips were dried at 37°C for an additional 1 h. During this time, the samples were prepared in saline with freshly thawed pre-pandemic collected plasma (Stem Cell Technologies) at a 1:50 ratio. All samples, excluding the no RBD control, had 1 μg RBD present in the final solution. SARS-CoV-2 NAb was added to three samples in increasing concentration: 0.05, 0.5, 5 μg, as well as 5 μg added to the no RBD control. Samples were all 70 μL in volume and incubated on ice for 1 h. The dried strips were laid on a 10° downward slope with the ACE2 end being the highest in elevation. Samples were added dropwise to the lower end of the strips and left to run for 15 min. The strips were then washed three times with TBST for 5 min each. Primary antibody (Mouse IgG2A-modified Anti-COVID-19 & SARS-CoV S glycoprotein [CR3022], Absolute Antibody) solution was made at a 1:1000 dilution in 3% BSA TBST buffer and added to the strips to incubate at 4°C overnight. The strips were washed three times again with TBST for 5 min each wash. Anti-mouse IgG-horseradish peroxidase conjugated secondary antibody (Cell Signaling Technologies) was diluted in 3% BSA TBST buffer at a 1:5000 dilution and applied to the strips to incubate for 1 h at 25°C. The strips were then washed three times again for 5 min each with TBST. ECL reagent was then mixed and applied to strips for 5 min before blotting off solution and imaging the strips on a Bio-Rad ChemiDoc XRS + system set to auto-exposure. Integrated density analysis of lateral flow strips was performed on ImageJ according to the ImageJ NIH Dot Blot Analysis tutorial, as described above.

Lateral flow assay cassette construction

Each lateral flow assay cassette is composed of an Ahlstrom 8964 fiber glass sample pad (22 × 3.9 mm; Ahlstrom-Munksjo), a Sartorius CN95 nitrocellulose membrane (25 × 3.9 mm; Sartorius, Germany) and an Ahlstrom 222 absorbent "sink" pad (20 × 3.9 mm; Ahlstrom-Munksjo), which were assembled sequentially onto a plastic-backed support card, such that there was an overlap of 2–5 mm between each pair of pads. Briefly, the nitrocellulose membrane and the sink pad were assembled first, after which the nitrocellulose membrane was striped twice, first with 0.47 mg of ACE-CBD, which served as the Infectious line, and then with 1.0 mg of recombinant protein A, which served as the Neutralized line (Figure 2A). The two proteins were dispensed 9 mm apart, such that the ACE2-CBD and the recombinant protein A (Sinobiological) were striped 34 and 25 mm, respectively, from the outer edge of the sink pad. For the second-generation version of the test that contains a third, more distal, line serving as a lateral flow run control, 1.0 mg of poly-L-lysine (Sigma) was striped onto the nitrocellulose membrane as well (Figure 4A). The striped nitrocellulose membrane was then dried at 50°C for 2 days. Finally, the sample pad was added, and the assembled strip was equipped with a Lohmann GL-422 clear cover-stock (45 × 3.9 mm; Lohmann Technologies), loaded into a plastic shell, and stored in a vacuum-sealed foil pouch under anhydrous conditions for future use.

Human sample processing

Blood samples from post-vaccination subjects were collected in heparinized collection tubes. Whole blood was immediately stored at −80°C. To collect plasma samples, whole blood was centrifuged at 2,000 × g for 10 min at 4°C, and plasma was collected, aliquoted and stored at −80°C. Upon receipt of commercially purchased human blood and plasma, samples were aliquoted and stored at −80°C. All assays performed in this study utilized blood and plasma thawed only once.

Lateral flow assay protocol

Frozen aliquots of the commercial and post-vaccination plasma samples were first thawed at room temperature and then placed on ice. Each plasma aliquot was then vortexed briefly for approximately 10 s, after which 1 μL of each sample was diluted 1:800 into room temperature LFA Run Buffer (Cataloid Products, Inc.) in a 1.5 mL microcentrifuge tube. Whole blood samples were diluted in similar fashion at the same ratio. The diluted samples were then mixed thoroughly by vortexing and incubated at room temperature for 10 min. Following this incubation period, 150 μL of each diluted sample was then transferred to a separate, new 1.5 mL microcentrifuge tube along with a single 5 mm circular-punched Ahlstrom 6615 colloidal gold pad to which recombinant RBD protein was conjugated (Cataloid Products, Inc). The tubes were subsequently placed in a microcentrifuge rack and left to incubate for 10 min at 25°C with continuous shaking at 200 rpm on a Model G2 Gyrotory Shaker (New Brunswick Scientific Co.). 75 μL of each RBD/colloidal gold-incubated plasma sample were then added to the sample well of a lateral flow assay test cassette and allowed to travel up the nitrocellulose membrane test strip by hydrodynamic force and capillary action. After 10 min, each sample pad was washed by adding 20 μL of running buffer (Cataloid Products, Inc.). Assay signals were allowed to develop for another 10 min, after which the test cassettes were placed in a shallow, ceiling-less Styrofoam box with constant, uniform overhead lighting and images immediately captured using a Fujifilm X-E2S digital camera (Fujifilm) at constant focus, aperture, and shutter speed settings. We also captured images immediately after this using the existing cameras on both a Galaxy S9 (Samsung) and iPhone X (Apple) under normal ambient laboratory lighting conditions with the cassette propped up vertically against a styrofoam box. The intensities of the signals at the Infectious and the Neutralized lines in the image taken from each test cassette were then quantified in ImageJ according to the

ImageJ NIH Dot Blot Analysis tutorial, as described above, without any background correction. The ratio of the intensities of the Neutralized line signal and the Infectious line signal (N/I ratio) was calculated for each sample to determine the NAb titer. Samples were in general run as a single replicate when sample volume was limiting, or as 5 replicates when assessing precision/reproducibility.

Pseudoviral neutralization assay

ACE2 expressing HEK293 cells (BPS Bioscience) were cultured in growth medium 1N culture media (BPS Bioscience) in 96-well white with transparent bottom plates. The day before the assay cells were seeded at a density of 10,000 cells/well in 100 μL of media and left to incubate at 37°C overnight. The following day assay samples were prepped by first thawing plasma samples on ice then diluting them at either 1:10, 1:100 or 1:10000 in 1N culture media (BPS Bioscience) with 1 μL of spike pseudotyped lentivirus with a luciferase reporter (BPS Bioscience) up to 10 μL. After a 30-min incubation period the plasma-pseudotype samples were added to the cells. The cells were then left to incubate for 48 h at 37°C with 5% CO_2. After 48 h, the ONE-Step luciferase reagent (BPS Bioscience) was prepared per the manufacturer's protocol and luminescence was measured on an Infinite m200 pro plate reader (Tecan). Neutralization ID_{50} titers were calculated using the "One-Site Fit LogIC50" regression function in Prism 8.0 (GraphPad). Samples were in general run as duplicates, or as a single replicate when sample volume was limiting.

Anti-spike IgG ELISA

96-well plates (Nunc MaxiSorp) were coated overnight at 4°C with recombinant spike protein S1 subunit (Biolegend) at a concentration of 1 μg/mL. Wells were subsequently blocked with phosphate buffered saline containing 5% bovine serum albumin. After washing, human plasma samples (1:200 dilution) were added and the plates were incubated for 2 h at 25 degrees Celsius. Horseradish peroxidase (HRP)-conjugated goat anti-human IgG (Southern Biotech; 1:1000 dilution) was added after washing and the plates were developed using TMB substrates (Biolegend). Absorbance at OD600 was measured using a Synergy HTX Reader (BioTek). Antibody units were determined based on a standard curve constructed using commercially available monoclonal human anti-spike protein antibodies (clone AM001414, Biolegend). Samples were in general run as a single replicate when sample volume was limiting, or as duplicates when assessing precision/reproducibility.

QUANTIFICATION AND STATISTICAL ANALYSIS

Statistical tests used, exact value of n, what n represents, and what dispersion and precision measures are used are found in the Figure Legends. Significance was defined as p value <0.05.

Sensitivity and specificity calculations

To assess and compare the performances of the LFA and the ELISA-based anti-spike IgG test at identifying plasma samples with specific neutralization titers, the sensitivity and specificity rates for a range of signal threshold values were determined for both tests in R (Version 3.5.2). This was done for neutralization ID_{50} titer cutoffs of 1:100, 1:200, 1:300 1:500, 1:700, and 1:1000, with specificity and sensitivity values being calculated for N/I ratios from 0 to 0.7, increasing in increments of 0.001, for the LFA, and for anti-spike IgG levels from 0 to 2430 mg/dL in increments of 5 mg/dL. The optimal signal threshold that would maximize both sensitivity and specificity for each test for a given neutralization titer cutoff was then determined using Microsoft Excel.

To calculate the sensitivity and specificity rates of either test for a given signal threshold, the following formulae were employed, using the specific pseudoviral neutralization assay ID_{50} titer cutoff:

$$Sensitivity\ Rate = \frac{Number\ of\ Samples\ with\ Test\ Signal \geq Threshold\ \&\ Neutralization\ ID_{50}\ Titer \geq Cutoff}{Total\ Number\ of\ Samples\ with\ Neutralization\ ID_{50}\ Titer \geq Cutoff}$$

$$Specificity\ Rate = \frac{Number\ of\ Samples\ with\ Test\ Signal < Threshold\ \&\ Neutralization\ ID_{50}\ Titer < Cutoff}{Total\ Number\ of\ Samples\ with\ Neutralization\ ID_{50}\ Titer < Cutoff}$$

To assess the diagnostic performance of the LFA test for measuring the loss of binding signal at the infectious line, the sensitivity and specificity values were calculated using just the integrated densities from the infectious line from the LFA test cassettes for the five different neutralization ID_{50} titers. These calculations were made for integrated density values between 15000 and 21000 in increments of 20 using the following formulae:

$$Sensitivity\ Rate = \frac{Number\ of\ Samples\ with\ Infectious\ Signal \leq Threshold\ \&\ Neutral.\ ID_{50}\ Titer \geq Cutoff}{Total\ Number\ of\ Samples\ with\ Neutralization\ ID_{50}\ Titer \geq Cutoff}$$

$$Specificity\ Rate = \frac{Number\ of\ Samples\ with\ Infectious\ Signal > Threshold\ \&\ Neutral.\ ID_{50}\ Titer < Cutoff}{Total\ Number\ of\ Samples\ with\ Neutralization\ ID_{50}\ Titer < Cutoff}$$

The optimal integrated density threshold that would maximize sensitivity and specificity of the test was determined in Microsoft Excel.

Receiver operating characteristic (ROC) curve generation

The calculated sensitivity and specificity values were used to generate receiver operating characteristic (ROC) curves for ID_{50} titer cutoffs of 1:100, 1:200, 1:300, 1:500, 1:700 and 1:1000. This was achieved by plotting the sensitivity rates as a function of the false positive (1-specificity) rates. The area under each ROC curve and its corresponding standard error were determined using the receiver operating curve functionality in Prism 8 (GraphPad). 95% confidence intervals for AUCs were calculated in NCSS Statistical Software (NCSS).

STATISTICAL ANALYSIS FOR COMPARING TWO ROC CURVES

To determine if the N/I ROC curve for a given ID_{50} neutralization titer cutoff was statistically different from the corresponding Spike IgG and loss of infectious signal ROC curves generated from the same set of patient samples, the method described by Hanley and McNeil was employed (Hanley and McNeil, 1983). Briefly, two different intermediate correlation coefficients were determined using the Pearson product-moment correlation method in GraphPad Prism 8. The first correlation coefficient, r_1, describes the correlation between the N/I values and the corresponding values from either the Spike IgG test or loss of infectious line signal analysis for patient samples with IC_{50} neutralization tires below the cutoff value. The second correlation coefficient, r_2, is for the values for patient samples with neutralization titers above the cutoff threshold from the two diagnostic methods being compared. A final correlation coefficient, r, which accounts for the correlation between the two areas of the ROC curves being compared, was then manually determined using the correlation coefficients table published in the paper mentioned previously. This table provides the correlation coefficient between two ROC areas, A_1 and A_2 as a function of the average correlation between the two pairs of ratings, $(r_1 + r_2)/2$, and the average area of the two ROC curves, $(A_1 + A_2)/2$. (*NB: If the average correlation,* $(r_1 + r_2)/2$, *was negative, the modulus was used).*

The critical ratio, z, was then calculated using the following formula:

$$z = \frac{A_1 - A_2}{\sqrt{SE_1^2 + SE_2^2 - 2rSE_1SE_2}}$$

where A_1 and SE_1 refer to the observed area and estimated standard error of the ROC area associated with the N/I ROC curve; A_2 and SE_2 refer to the corresponding quantities for either the Spike IgG ROC curve or the Loss of I ROC curve; and r represents the estimated correlation between A_1 and A_2. The resulting critical value was then used to calculate a two-tail p value using the following Microsoft Excel function:

$$= 2 * (1 - NORMSDIST(z))$$